Immobilized Laccase on Bentonite-derived Mesoporous Materials for Removal of Tetracycline

Xiaofeng Wen [a,1], Zhuotong Zeng[b,1], Chunyan Du [c,1], Danlian Huang [a,1], Guangming Zeng[a,*], Rong Xiao[b,*], Cui Lai[a], Piao Xu [a], Chen Zhang [a], Jia Wan [a], Liang Hu [a], Lingshi Yin [c], Chengyun Zhou [a], Rui Deng [a]

[a] *College of Environmental Science and Engineering, Hunan University and Key Laboratory of Environmental Biology and Pollution Control (Hunan University), Ministry of Education, Changsha 410082, P.R. China;*

[b] *Department of Dermatology, Second Xiangya Hospital, Central South University, Changsha 410011, P R China;*

[c] *School of Hydraulic Engineering, Changsha University of Science &Technology and Key Laboratory of Water-Sediment Sciences and Water Disaster Prevention of Hunan Province, Changsha 410114, P.R. China.*

* Corresponding author.

E-mail address: zgming@hnu.edu.cn (G.M.Zeng), xiaorong65@csu.edu.cn (R. Xiao).

[1] These authors contribute equally to this article

ABSTRACT: Bentonite is a natural and environmentally clay mineral, and bentonite-derived mesoporous materials (BDMMs) were obtained conveniently from the alkali and acid treatment of bentonite. In the present study, BDMMs were explored for immobilization of laccase obtained from *Trametes versicolor*. As a result, bentonite-derived mesoporous materials-*Laccase* (BDMMs-*Lac*) was developed for the removal of tetracycline (TC). The enzyme immobilization process was carried out through physical adsorption contact (ion exchange adsorption, hydrogen bond adsorption, and Van der waals adsorption) between the BDMMs and laccase. The process of immobilization remarkably increased its operating temperature. The BDMMs-*Lac* exhibited over 60% removal efficiency for TC within three hours in the presence of 1-hydroxybenzotriazole (HBT). In conclusion, BDMMs-*Lac* showed more promising potential than free laccase for practical continuous applications.

Keywords: Bentonite-derived mesoporous materials, Laccase, Physisorption Immobilization, Tetracycline, Catalysis

1. Introduction

Laccase (EC 1.10.3.2) is an oxidoreductase that belongs to the multicopper oxidase protein family (Huang et al., 2017; Madhavi and Lele, 2009; Zhang et al., 2014). Laccase has the ability to catalyze some substrates to water (Spina et al., 2015; Huang et al., 2016). In the presence of small molecular weight mediators, laccase has more extensive substrate range and thus exhibits wider applicability in polluted water (Cheng et al., 2016; Chen et al., 2016; Rodriguez and Toca, 2006). The use of laccases also offers a method that is free from secondary pollution during actual wastewater treatment (Lai et al., 2016; Liu et al., 2013; Monje et al., 2010). However, the low stability and high production costs of laccase limit its applicability (Ashe et al., 2016; Li et al., 2018).

Immobilization can overcome the limits of laccase application by enhancing the enzyme properties (Mohamad et al., 2015; Cheng et al., 2016). The immobilization methods of laccase have been explored for years (Deng et al., 2013; Guzik et al., 2014; Zhou et al., 2018). Immobilization can increase the stability of enzymes and thus improve the operability of laccase in practice (Lai et al., 2019; Sheldon and van Pelt, 2013). Multifarious carriers have been studied for the successful immobilization of

laccase (Zhou et al., 2013; Liu et al., 2012). Clays are low-cost, eco-friendly, recyclable, have low mass transfer, and demonstrate microbial corrosion resistance capacity (An et al., 2015; Li et al., 2015; Liang et al., 2017; Wu et al., 2017). Through activation or etching, they can attain highly specific surface areas and numerous functional groups (Gong et al., 2009; Osuna et al., 2018; Shu et al., 2016; Zeng et al., 2017).

Bentonite, which has layered structure with cations such as Na^{+} or Ca^{2+}, shows promising and highly suitable application for the loading of an extensive range of biomolecules (Liang et al., 2017; Ghiaci et al., 2009; Ma et al., 2018). After etching, bentonite exhibited highly improved characteristics, including those relation to cation exchange capacity and surface area (Liang et al., 2017; Bajpai and Sachdeva, 2002; Shu et al., 2014). Furthermore, bentonite, as a natural mineral, is eco-friendly, inexpensive, and accessible (Long et al., 2011; Issaabadi et al., 2017). The application of bentonite for enzyme immobilization has been studied by several research groups (Salem and Salem, 2017; Andjelkovi et al., 2015). Conversely, the utilization of mesoporous and high surface area bentonite for the immobilization of laccase and other different biocatalysts remains to be explored (Xu et al., 2012; Andjelkovi et al., 2015; Zhou et al.,

62 2018).

63 Antibiotic pollution has become of increasing environmental concern (Manaia et
64 al., 2016). Antibiotics are widely utilized to treat diseases caused by various bacterial or
65 pathogenic microbes, however, their Misuse and over accumulation threaten the
66 environment (Liu et al., 2016; Polesel et al., 2016). Tetracycline (TC) is one of the most
67 widely used antibiotics (Nasseh et al., 2018; Gothwal and Shashidhar, 2015). The poor
68 degradation of TC from traditional municipal wastewater treatment plants has led to a
69 latent negative impact on aquatic organisms, thus necessitating the exploration of
70 treatment technologies (Halling-Sørensen, 2001; Huang et al., 2017; Tan et al., 2015).
71 Among the numerous treatment methods, the biodegradation of TC by laccase or
72 immobilized laccase is effective (Rojas-Espinoza et al., 2018; Xu et al., 2012).

73 Although modified bentonite materials have been frequently applied to immobilize
74 enzymes, the use of mesoporous and high surface area bentonite for laccase
75 immobilization has not been explored (Andjelkovi et al., 2015; Ghiaci et al., 2009; Liu
76 et al., 2012). Bentonite can be modified to be mesoporous and to possess a high surface
77 area (Toor et al., 2015; Önal and Sarıkaya, 2007). NaOH-HCl etching modification is an
78 alkali/acid activation composite modification process (Önal and Sarıkaya, 2007). This

method has been utilized for the etching of clay materials such as Halloysite, Kaolinite, from wich mesoporous materials have successfully obtained (Li et al., 2015; Zhou et al., 2014). However, the use of alkali/acid activation composite modification for bentonite has not been explored. Thus, in this study, bentonite-derived mesoporous materials (BDMMs) were constructed by NaOH-HCl etching. The BDMMs were utilized for laccase immobilization to obtain bentonite-derived mesoporous materials-Laccase (BDMMs-Lac), and the characteristics of BDMMs and the treatment capacity of BDMMs-Lac were explored. BDMMs-Lac was applied for TC antibiotic removal in the presence of the redox mediator 1-hydroxybenzotriazole (HBT). This study is aimed at establishing new eco-friendly, low-cost, and re-usable carriers for immobilizing laccase and for exploring the treatment capacity and removal ability of immobilized laccase for emerging antibiotic pollutants.

2. Material and methods

2.1. Materials

Laccase (≥ 0.5 U mg^{-1}) from *Trametes versicolor*, HBT, TC, and 2, 2-azino-bis (3-ethylbenzothiazoline-6-sulfonic acid) (ABTS) were obtained from Sigma-Aldrich (St. Louis, MO, USA). Bentonite was provided by Sinopharm Chemical Reagent Co. Ltd.

(Shanghai, China). All of the other chemicals were of analytical grade.

2.2. Etching of the Bentonite

Pristine bentonite was added to NaOH (6 M) and stirred. The bentonite was then washed five times with ultrapure water, dried at 383 K for 12 h, and then added to HCl (5 M) at 353 K with constant stirring for 6 h. The above material was then washed and dried to obtain BDMMs.

2.3. Laccase Activity Assays

Laccase activity was tested using ABTS as a substrate (Zhang et al., 2014). Briefly, the assay compound consisted of 0.1 M citrate buffer (pH=5), 1 mM ABTS and free laccase or BDMMS-*Lac* samples. The activity of BDMMS-Lac and free laccase was detected at an absorbance of 420 nm (UV-2250, Shimadzu Corp., Japan). One unit of laccase activity was defined as the amount of BDMMS-*Lac* or free laccase required to oxidize 1 μM of substrate per minute.

2.4. Laccase Immobilization

The BDMMs was suspended in citrate phosphate buffer (0.1 M, pH=3-8) containing laccase (0.5-4 mg/mL). The mixtures were then incubated. Later, the sample was centrifuged and the bottom solid was collected and washed several times with

citrate buffer (0.1 M, pH=5). The final solid BDMMs-*Lac* was obtained after freeze drying at 173 K for 12 h. Fig. 1 depicts the typical process for the stepwise etching of pristine bentonite, and the adsorption loading of laccase.

Fig. 1. Schematic of BDMMs preparation and succeeding laccase physisorption immobilization on BDMMs.

2.5. Stability Assessment

2.5.1. Thermal Stability

For temperature stability, free laccase and immobilized laccase were added to centrifuge tubes containing citrate buffer (pH=5) and were maintained at 303 K to 353 K for 120 min. They reacted with the ABTS and were centrifuged and then measured at 420 nm (UV-2250, SHimadzu Corp.).

2.5.2. Reusability of Immobilized Laccase

The BDMMs-*Lac* was dispersed in citrate-phosphate buffer (pH 5) containing 1 mM ABTS and then incubated at 303 K. The sample was centrifuged (6,570 ×g) and the concentration of the transformed ABTS was measured. The BDMMs-*Lac* was washed with citrate-phosphate buffer. The above procedure was repeated for 10 cycles.

2.6. Immobilized Laccase System for the Removal of TC

The effect of parameters such as BDMMs-*Lac* dosage (0.5–4 mg/mL) and reaction time (10–180 min) were studied. The reaction mixture containing BDMMs-*Lac* and 10 mg/L of TC solution was placed at 303 K for 120 min. TC was tested at the absorbance of 360 nm (UV-2250, Shimadzu Corp.). All of the experiments were examined in triplicate. To determine the possible removal of TC due to adsorption onto the BDMMs, heated-devitalized BDMMs-*Lac* was used to remove the TC.

3. Results and Discussion

3.1. Structural Characterization

The morphologies of the bentonite, BDMMs, and BDMMs-Lac samples are presented on Scanning Electron Microscopy (SEM) images (Fig. 2). The Fig. 2 (a) illustrates the unbroken structure of the crude bentonite, which consisted of homogeneous particles. Fig. 2 (b) indicates the etching appearance of BDMMs whereby the integrated particles were visually damaged and the interlamellar spacing was enlarged. Relevant Energy dispersive spectroscopic (EDS) analysis confirmed that no obvious elemental change occurred after etching (Fig. 2 (b)). Fig. 2 (c) and Fig. 2 (d) showed no alteration in the structure of BDMMs-Lac before or after degradation in

146 comparison with BDMMs.

147 The N_2 adsorption-desorption curves of the samples are presented in Fig. 3A. The
148 values of BDMMs were highly elevated in contrast to that of original bentonite. The
149 plot style also changed from III style (H3 hysteresis loop) to V style (H4 hysteresis loop)
150 (Zhang et al., 2016; Yu and Zhang, 2010). The hysteresis loop showed that both
151 bentonite and BDMMs consisted of slit holes, which were formed by the accumulation
152 of flaky particles or layered structures (Yang et al., 2010; Chen et al., 2017). The BET
153 results indicated that the pristine bentonite had a surface area equal to 3.30 m^2/g, a pore
154 size equal to 2.73 nm and a pore volume equal to 22.46 mm^3/g. Meanwhile, the surface
155 area of BDMMs was 244.62 m^2/g, the pore size was 5.53 nm, and the pore volume was
156 338.8 mm^3/g. The specific surface areas were higher than that detected in previous
157 researches (Bajpai and Sachdeva, 2002; Ghiaci et al., 2009).

158 The Fig. 3B shows the FTIR spectra of bentonite, BDMMs, BDMMs-*Lac*, and
159 BDMMs-*Lac* after degradation. The broad adsorption band around 3438 cm^{-1} among all
160 of the samples could be attributed to the stretching vibration of O-H caused by water
161 molecules that are present in the hydrogen bonded interlayer (Jiang et al., 2018; Ztrk et
162 al., 2008). The adsorption band at 1637 cm^{-1} in all of the samples indicates the

stretching vibration of crystal water molecules in the lattice (Ztrk et al., 2008). The band at 1429 cm^{-1} was presumed to represent the symmetric stretching vibration absorption peak of –COOH (Wen et al., 2019; Chen et al., 2017; Tang et al., 2014). The absorption bands around 1027 and 696 cm^{-1} of spectrum a, b, c and d were caused by the bending vibration of Si-O-Si and Si-O, respectively (Huang et al., 2016; Ztrk et al., 2008). However, the band at 3627 cm^{-1} was interpreted as the stretching vibration of O-H due to the existence of interlayered adsorption water molecules that disappeared after etching (Huang et al., 2015). The same phenomenon was also observed in the peaks of 2352, 829, and 462 cm^{-1}. The presence of narrow bands at 2352 cm^{-1} might correspond to the impurities mixed in the bentonite. The other bands in the range of 500-800 cm^{-1} were the lattice vibration of M-O, M-O-M, and O-M-O (Andjelkovi et al., 2015). Their changes among the different curves may be attributed to the ion exchange and regent reaction during the etching process (Li et al., 2015).

The X-ray diffraction (XRD) patterns of the bentonite and BDMMs are displayed in Fig. 3C. The characteristic reflection of bentonite at 5.8 °belonged to montmorillonite (Chen et al., 2017). It was disappeared after etching. The reductions in BDMMs may be due to the activation of etching regents. The basal space reflections presented a sharp

peak at 2θ = 26.64° in the XRD spectrum of the bentonite and BDMMs samples and indicated a (101) basal spacing of 1.54 nm (JCPDS Card No. 46-1045) (Toor et al., 2015). The characteristic XRD peaks for quartz (2θ= 26.64°, 42.45°, 68.32°), marked by their indices (101), (200), (301), were almost identical between the bentonite and BDMMs. No obvious shifts in the characteristic peaks of the bentonite and BDMMs were observed, demonstrating that there was no expansion in interlamellar spacing. Thus, the same XRD patterns of the bentonite and BDMMs confirmed that they possessed the same crystal structure and interplanar spacing.

Fig. 2. SEM images and related EDS of a) bentonite, b) BDMMs, c) BDMMs-Lac, and d) BDMMs-Lac after TC degradation.

Fig.3. A) BET nitrogen adsorption/desorption plots of the bentonite and BDMMs. B) FT-IR spectra of bentonite, BDMMS, BDMMS-*Lac*, and BDMMs-*Lac* after degradation. C) XRD curves of the bentonite and BDMMs.

3.2. Optimum Conditions of Laccase Immobilization

Immobilization using bentonite as a support material is influenced by many factors (Liu et al., 2012). As shown in Fig. 4A, when the initial laccase concentration increased from 0.5 to 4 mg/mL, the loaded laccase on the bentonite also increased. However, the

activity of the immobilized laccase only increased until 2 mg/mL. When the laccase concentration exceeded 2 mg/mL, a decrease in the activity recovery of BDMMs-*Lac* was observed. Some similar observations have been made in previous studies (Kadam et al., 2017). This phenomenon could be attributed to the overloading of laccase on supports, as the overloading of laccase on the surface of the supports would result in the congestion or crowding of the laccase molecules (Liu et al., 2012). Diffusion-controlled limitations appeared when the laccase loading was high. The agglomeration or crowding of laccase also resulted in the conformational change of the laccase molecules, and a suitable laccase concentration was found to be important for maintaining laccase activity. Thus the optimum laccase concentration was set as 2 mg/mL for the subsequent analyses.

As depicted in Fig. 4B, the activity and the relative activity of BDMMs-Lac changed with the increase in immobilization time from 15 to 180 min. The relative activity of BDMMs-*Lac* increased remarkably until 30 min, following which the relative activity remained the same from 30 to 120 min. The activity of BDMMs-*Lac* almost reached 800 U/g, following which the activity and relative activity began to decline. The activity of the immobilized enzymes depends on the nature of the enzyme

protein (Liu et al., 2012). As time progressed, the possible amounts of inactivated laccase increased during immobilization, and the laccase flexibility declined. With the increase in physical adsorption immobilization time, the adsorption site on BDMMs was eliminated. The relevant steric hindrance and diffusion limitations might have also resulted in the decrease in laccase activity (Liu et al., 2012).

The effect of solution pH on the activity of free and BDMMs-*Lac* was explored at different pH values ranging from 3.0 to 8.0 (Fig. 4C). The free and immobilized laccase typically demonstrated maximal activity at pH 4.0 and pH 5.0. The variation in optimum pH was also previously surveyed in immobilized laccase on magnetic bimodal mesoporous carbon (Liu et al., 2012). It may be attributed to the electrostatic interaction affected by the support microenvironment around the laccase. Different pH values resulted in different microenvironments. The isoionic point influenced the net charge of the laccase and carrier such that the laccase activity could be hindered or invoked (Chen et al., 2015; Liu et al., 2012; Zhang et al., 2015). BDMMs-*Lac* showed better adaptability when the pH value was above 5. As the pH increased to 6, the free laccase and BDMMs-*Lac* maintained 37% and 48% of their relative activity, respectively. To a certain extent, this result indicated that immobilization could retain laccase activity.

Fig. 4. A) Effect of laccase concentrations from 0.5 mg/mL to 4 mg/mL on the activity of the immobilized laccase. B) Effect of time from 15 min to 180 min on the activity of the immobilized laccase. C) Effect of pH from 3.0 to 8.0 on the activity of the free and immobilized laccase.

3.3. Properties of BDMMs-Lac

Operational stability is important for determining processing costs (Liu et al., 2012). The results presented in Fig. 5A showed that BDMMs-*Lac* lost 37% and 64% of its original activity after three and five cycles, respectively. The physical adsorption immobilization exhibited weak binding forces between enzyme and carrier. Thus, the activity loss may have resulted from the laccase leaching during the washing stages (Skoronski et al., 2017).

The thermostability of free laccase and BDMMs-*Lac* was explored over a temperature range of 303 K to 353 K. As indicted in Fig. 5B, BDMMs-*Lac* was more stable than the free laccase, and both free laccase and BDMMs-*Lac* presented their highest stability at 313 K. Furthermore, between 323 K and 353 K, the immobilized laccase maintained 96% of its initial activity, while free laccase could only retain 0.54% of its initial activity when the temperature exceeded 343 K. The results were attributed to the high thermostability of BDMMs-*Lac* towards denaturation. Immobilization

248 increased laccase rigidity and decreased laccase conformational flexibility (Andjelkovi
249 et al., 2015). The highly improved thermal stability of BDMMs-*Lac* benefits its
250 application in high-temperature industrial processes (Menezes-Blackburn et al., 2011).

251 **Fig. 5**. A) Operational stability of BDMMs-*Lac* in continuous cycles. B) Thermal stability studies of
252 free laccase and BDMMs-*Lac* at 303-353 K for up to 120 min.

253 *3.4. Removal of TC*

254 The effect of reaction time on removal of TC is displayed in Fig. 6A. The removal
255 of TC could be attributed to the combined effects of degradation by BDMMs-Lac and
256 the adsorption by the BDMMs support. As shown in Fig. 6A, approximately 60% of the
257 TC was removed in 120 min by BDMMs-*Lac*. The more important contribution of the
258 laccase catalytic process could thus be confirmed, as the adsorption only contributed
259 approximately 20% of the removal. However, the result also revealed the benefit of
260 employing BDMMs as immobilization support in the removal process. The
261 accumulation of the catabolite might inhibit the removal process, which was reported in
262 a previous study (Yang et al., 2017).

263 The relationship between immobilized laccase dosage and TC removal is presented
264 in Fig. 6B. The removal efficiency of TC gradually increased with increased in

265 immobilized laccase dosage from 0.4 to 4 mg/mL. When the dosage was 4 mg/mL, the
266 removal efficiency reached 52%. When the dosage was 2 mg/mL, the removal amount
267 reached 1.85 mg/g. The removal efficiency began to decrease when the BDMMs-Lac
268 dosage was higher than 4 mg/mL, and this phenomenon was attributed to excessive
269 dosage, leading to contact site reduction between TC and mediator HBT, as well as
270 contributing to the consumption of laccase activity (Sun et al., 2017).

271 **Fig. 6**. A) Time-course of the removal and adsorption rates for TC by BDMMs-*Lac* and the
272 heated-devitalized BDMMs-*Lac*. B) Effect of immobilized laccase dosage on the removal rates of
273 TC by BDMMs-*Lac*.

274 **4. Conclusions**

275 The surface area, average pore size, and pore volume of BDMMs obtained from
276 this study were all increased (8.3→244.62 m^2/g, 2.73→5.53 nm, 22.46→338.8 mm^3/g).
277 The stability of BDMMs-*Lac* was improved compared to free laccase, particularly
278 thermal stability. The biodegradation rate of BDMMs-*Lac* for TC reached nearly 60%.
279 This study showed that BDMMs could be conveniently and efficiently obtained and has
280 potential applicability in further practical biomacromolecule immobilization.
281 Furthermore, as the obtained BDMM-*Lac* is an economical and eco-friendly biocatalyst,

it has wide applicability for the elimination of micropollutants from wastewater.

Acknowledgements

This study was financially supported by the Program for the National Natural Science Foundation of China (81773333, 51109016, 51278176, 51408206, 51879101, 51579098, 51779090, 51709101, 51521006, 51809090, 51378190), the National Program for Support of Top-Notch Young Professionals of China (2014), The Natural Science Foundation of Hunan province (2018JJ2349), Hunan Water Conservancy Science and Technology Project ([2016]194-12, [2017]230-22), the Fundamental Research Funds for the Central Universities (531109200027, 531107051080, 531107050978), the Hunan Provincial Science and Technology Plan Project (2017SK2361, 2016RS3026, 2018SK20410, 2017SK2243, 2016RS3026), the Program for New Century Excellent Talents in University (NCET-13-0186), the Program for Changjiang Scholars and Innovative Research Team in University (IRT-13R17), the Scientific Research Fund of Hunan Provincial Education Department (No.521293050).

References

Ali, M.M.M., Ahmed, M.J., Hameed, B.H., 2018. NaY zeolite from wheat (Triticum

aestivum L.) straw ash used for the adsorption of tetracycline. J. Clean. Prod. 172, 602-608.

An, N., Zhou, C.H., Zhuang, X.Y., Tong, D.S., Yu, W.H., 2015. Immobilization of enzymes on clay minerals for biocatalysts and biosensors. Appl. Clay Sci. 114, 283-296.

Andjelkovi, U., Milutinovi Nikoli, A., Jovi Jovi I, N.A., Bankovi, P., Bajt, T., Mojovi, Z., Vuj I, Z., Jovanovi, D.A., 2015. Efficient stabilization of Saccharomyces cerevisiae external invertase by immobilisation on modified beidellite nanoclays. Food Chem. 168, 262-269.

Ashe, B., Nguyen, L.N., Hai, F.I., Lee, D.J., van de Merwe, J.P., Leusch, F.D.L., Price, W.E., Nghiem, L.D., 2016. Impacts of redox-mediator type on trace organic contaminants degradation by laccase: Degradation efficiency, laccase stability and effluent toxicity. International Biodeterioration and Biodegradation. 113, 169-176.

Bajpai, A.K., Sachdeva, R., 2002. Immobilization of diastase onto acid-treated bentonite clay surfaces. Colloid & Polymer Science. 280, 892-899.

Chen, M., Xu, P., Zeng, G., Yang, C., Huang, D., Zhang, J., 2015. Bioremediation of soils contaminated with polycyclic aromatic hydrocarbons, petroleum, pesticides,

317 chlorophenols and heavy metals by composting: Applications, microbes and future
318 research needs. Biotechnol. Adv. 33, 745-755.
319 Chen, Y., Peng, J., Xiao, H., Peng, H., Bu, L., Pan, Z., He, Y., Chen, F., Wang, X., Li,
320 S., 2017. Adsorption behavior of hydrotalcite-like modified bentonite for Pb^{2+}, Cu^{2+}
321 and methyl orange removal from water. Appl. Surf. Sci. 420, 773-781.
322 Chen, Y.Y., Stemple, B., Kumar, M., Wei, N., 2016. Cell Surface Display Fungal
323 Laccase as a Renewable Biocatalyst for Degradation of Persistent Micropollutants
324 Bisphenol A and Sulfamethoxazole. Environ. Sci. Technol. 50, 8799-8808.
325 Cheng, M., Zeng, G., Huang, D., Lai, C., Xu, P., Zhang, C., Liu, Y., 2016. Hydroxyl
326 radicals based advanced oxidation processes (AOPs) for remediation of soils
327 contaminated with organic compounds: A review. Chem. Eng. J. 284, 582-598.
328 Cheng, Y., He, H., Yang, C., Zeng, G., Li, X., Chen, H., Yu, G., 2016. Challenges and
329 solutions for biofiltration of hydrophobic volatile organic compounds. Biotechnol.
330 Adv. 34, 1091-1102.
331 Deng, J., Zhang, X., Zeng, G., Gong, J., Niu, Q., Liang, J., 2013. Simultaneous removal
332 of Cd(II) and ionic dyes from aqueous solution using magnetic graphene oxide
333 nanocomposite as an adsorbent. Chem. Eng. J. 226, 189-200.

334 Ghiaci, M., Aghaei, H., Soleimanian, S., Sedaghat, M.E., 2009. Enzyme immobilization:
335 Part 2. Immobilization of alkaline phosphatase on Na-bentonite and modified
336 bentonite. Appl. Clay Sci. 43, 308-316.
337 Gong, J.L., Wang, B., Zeng, G.M., Yang, C.P., Niu, C.G., Niu, Q.Y., Zhou, W.J., Liang,
338 Y., 2009. Removal of cationic dyes from aqueous solution using magnetic multi-wall
339 carbon nanotube nanocomposite as adsorbent. J. Hazard. Mater. 164, 1517-22.
340 Gong, X., Huang, D., Liu, Y., Zeng, G., Wang, R., Wan, J., Zhang, C., Cheng, M., Qin,
341 X., Xue, W., 2017. Stabilized Nanoscale Zerovalent Iron Mediated Cadmium
342 Accumulation and Oxidative Damage ofBoehmeria nivea (L.) Gaudich Cultivated in
343 Cadmium Contaminated Sediments. Environ. Sci. Technol. 51, 11308-11316.
344 Gothwal, R., Shashidhar, T., 2015. Antibiotic Pollution in the Environment: A Review.
345 CLEAN-Soil Air Water. 43, 479-489.
346 Guzik, U., Hupert-Kocurek, K., Wojcieszyska, D., 2014. Immobilization as a Strategy
347 for Improving Enzyme Properties-Application to Oxidoreductases. Molecules. 19,
348 8995-9018.
349 Halling-Sørensen, G.S.B., 2002. Toxicity of Tetracyclines and Tetracycline
350 Degradation Products to Environmentally Relevant Bacteria, Including Selected

Tetracycline-Resistant Bacteria. Arch. Environ. Con. Tox. 42, 263-271.

Huang, D., Gong, X., Liu, Y., Zeng, G., Lai, C., Bashir, H., Zhou, L., Wang, D., Xu, P., Cheng, M., Wan, J., 2017. Effects of calcium at toxic concentrations of cadmium in plants. Planta. 245, 863-873.

Huang, D., Hu, C., Zeng, G., Cheng, M., Xu, P., Gong, X., Wang, R., Xue, W., 2016. Combination of Fenton processes and biotreatment for wastewater treatment and soil remediation. Sci. Total Environ. 574, 1599-1610.

Huang, D., Liu, L., Zeng, G., Xu, P., Huang, C., Deng, L., Wang, R., Wan, J., 2017. The effects of rice straw biochar on indigenous microbial community and enzymes activity in heavy metal-contaminated sediment. Chemosphere. 174, 545-553.

Huang, D., Wang, R., Liu, Y., Zeng, G., Lai, C., Xu, P., Lu, B., Xu, J., Wang, C., Huang, C., 2015. Application of molecularly imprinted polymers in wastewater treatment: a review. Environ. Sci. Pollut. R. 22, 963-977.

Huang, D., Xue, W., Zeng, G., Wan, J., Chen, G., Huang, C., Zhang, C., Cheng, M., Xu, P., 2016. Immobilization of Cd in river sediments by sodium alginate modified nanoscale zero-valent iron: Impact on enzyme activities and microbial community diversity. Water Res. 106, 15-25.

368 Islas-Espinoza, M., Aydin, S., Heras, A.D.L., Ceron, C.A., Martínez, S.G.,
369 Vázquez-Chagoyán, J.C., 2018. Sustainable bioremediation of antibacterials, metals
370 and pathogenic DNA in water. J. Clean. Prod. 183, 112-120.
371 Issaabadi, Z., Nasrollahzadeh, M., Sajadi, S.M., 2017. Green synthesis of the copper
372 nanoparticles supported on bentonite and investigation of its catalytic activity. J.
373 Clean. Prod. 142, 3584-3591.
374 Jiang, C., Yin, L., Wen, X., Du, C., Wu, L., Long, Y., Liu, Y., Ma, Y., Yin, Q., Zhou, Z.,
375 Pan, H., 2018. Microplastics in Sediment and Surface Water of West Dongting Lake
376 and South Dongting Lake: Abundance, Source and Composition. Int. J. Env. Res.
377 Pub. He. 15, 2164.
378 Kadam, A.A., Jang, J., Lee, D.S., 2017. Supermagnetically Tuned Halloysite Nanotubes
379 Functionalized with Aminosilane for Covalent Laccase Immobilization. ACS Appl.
380 Mater. Inter. 9, 15492-15501.
381 Križnik, L., Vasić, K., Knez, Ž., Leitgeb, M., 2018. Hyper-activation of ß-galactosidase
382 from Aspergillus oryzae via immobilization onto amino-silane and chitosan
383 magnetic maghemite nanoparticles. J. Clean. Prod. 179, 225-234.
384 Lai, C., Wang, M., Zeng, G., Liu, Y., Huang, D., Zhang, C., Wang, R., Xu, P., Cheng,

M., Huang, C., Wu, H., Qin, L., 2016. Synthesis of surface molecular imprinted TiO_2/graphene photocatalyst and its highly efficient photocatalytic degradation of target pollutant under visible light irradiation. Appl. Surf. Sci. 390, 368-376.

Lai, C., Zhang, M., Li, B., Huang, D., Zeng, G., Qin, L., Liu, X., Yi, H., Cheng, M., Li, L., Chen, Z., Chen, L., 2019. Fabrication of CuS/$BiVO_4$ (0 4 0) binary heterojunction photocatalysts with enhanced photocatalytic activity for Ciprofloxacin degradation and mechanism insight. Chem. Eng. J. 358, 891 - 902.

Lee, S.J., Lee, J.H., Yang, X., Yoo, H.Y., Han, S.O., Park, C., Kim, S.W., 2017. Re-utilization of waste glycerol for continuous production of bioethanol by immobilized Enterobacter aerogenes. J. Clean. Prod. 161, 757-764.

Li, B., Lai, C., Zeng, G., Qin, L., Yi, H., Huang, D., Zhou, C., Liu, X., Cheng, M., Xu, P., Zhang, C., Huang, F., Liu, S., 2018. Facile Hydrothermal Synthesis of Z-Scheme Bi2Fe4O9/Bi2WO6 Heterojunction Photocatalyst with Enhanced Visible Light Photocatalytic Activity. ACS Appl Mater Interfaces. 10, 18824-18836.

Li, T., Shu, Z., Zhou, J., Chen, Y., Yu, D., Yuan, X., Wang, Y., 2015. Template-free synthesis of kaolin-based mesoporous silica with improved specific surface area by a novel approach. Appl. Clay Sci. 107, 182-187.

Liang, J., Yang, Z., Tang, L., Zeng, G., Yu, M., Li, X., Wu, H., Qian, Y., Li, X., Luo, Y., 2017. Changes in heavy metal mobility and availability from contaminated wetland soil remediated with combined biochar-compost. Chemosphere. 181, 281-288.

Liu, J., Cai, Y., Liao, X., Huang, Q., Hao, Z., Hu, M., Zhang, D., Li, Z., 2013. Efficiency of laccase production in a 65-L air-lift reactor for potential green industrial and environmental application. J. Clean. Prod. 39, 154-160.

Liu, J., Luo, Q., Huang, Q., 2016. Removal of 17β -estradiol from poultry litter via solid state cultivation of lignolytic fungi. J. Clean. Prod. 139, 1400-1407.

Liu, Y.Y., Zeng, Z.T., Zeng, G.M., Tang, L., Pang, Y., Li, Z., Liu, C., Lei, X.X., Wu, M.S., Ren, P.Y., Liu, Z.F., Chen, M., Xie, G.X., 2012. Immobilization of laccase on magnetic bimodal mesoporous carbon and the application in the removal of phenolic compounds. Bioresource Technol. 115, 21-26.

Long, F., Gong, J., Zeng, G., Chen, L., Wang, X., Deng, J., Niu, Q., Zhang, H., Zhang, X., 2011. Removal of phosphate from aqueous solution by magnetic Fe‐Zr binary oxide. Chem. Eng. J. 171, 448-455.

Ma, J., Amjad Bashir, M., Pan, J., Qiu, L., Liu, H., Zhai, L., Rehim, A., 2018.

Enhancing performance and stability of anaerobic digestion of chicken manure using thermally modified bentonite. J. Clean. Prod. 183, 11-19.

Madhavi, V., Lele, S.S., 2009. Laccase: Properties and Applications. BioResources. 4, 1694-1717.

Manaia, C.M., Macedo, G., Fatta-Kassinos, D., Nunes, O.C., 2016. Antibiotic resistance in urban aquatic environments: can it be controlled? Appl. Microbiol. Biot. 100, 1543-1557.

Menezes-Blackburn, D., Jorquera, M., Gianfreda, L., Rao, M., Greiner, R., Garrido, E., 2011. Activity stabilization of Aspergillus niger and Escherichia coli phytases immobilized on allophanic synthetic compounds and montmorillonite nanoclays. Bioresource Technol. 102, 9360-9367.

Mohamad, N.R., Marzuki, N.H.C., Buang, N.A., Huyop, F., Wahab, R.A., 2015. An overview of technologies for immobilization of enzymes and surface analysis techniques for immobilized enzymes. Biotechnol. Biotec. Eq. 29, 205-220.

Monje, P.G., Gonzalez-Garcia, S., Moldes, D., Vidal, T., Romero, J., Moreira, M.T., Feijoo, G., 2010. Biodegradability of kraft mill TCF biobleaching effluents: Application of enzymatic laccase-mediator system. Water Res. 44, 2211-2220.

436 Nasseh, N., Taghavi, L., Barikbin, B., Nasseri, M.A., 2018. Synthesis and
437 characterizations of a novel FeNi3/SiO2/CuS magnetic nanocomposite for
438 photocatalytic degradation of tetracycline in simulated wastewater. J. Clean. Prod.
439 179, 42-54.
440 Önal, M., Sarıkaya, Y., 2007. Preparation and characterization of acid-activated
441 bentonite powders. Powder Technol. 172, 14-18.
442 Osuna, F.J., Cota, A., Pavón, E., Alba, M.D., 2018. A comprehensive and in-depth
443 analysis of the synthesis of advanced adsorbent materials. J. Clean. Prod. 194,
444 665-672.
445 Polesel, F., Andersen, H.R., Trapp, S., Plosz, B.G., 2016. Removal of Antibiotics in
446 Biological Wastewater Treatment Systems-A Critical Assessment Using the
447 Activated Sludge Modeling Framework for Xenobiotics (ASM-X). Environ. Sci.
448 Technol. 50, 10316-10334.
449 Rodriguez, C.S., Toca, H.J., 2006. Industrial and biotechnological applications of
450 laccases: a review. Biotechnol. Adv. 24, 500-13.
451 Salem, S., Salem, A., 2017. A novel design for clean and economical manufacturing
452 new nano-porous zeolite based adsorbent by alkali cement kiln dust for lead uptake

from wastewater. J. Clean. Prod. 143, 440-451.

Sheldon, R.A., van Pelt, S., 2013. Enzyme immobilisation in biocatalysis: why, what and how. Chem. Soc. Rev. 42, 6223-6235.

Shu, Z., Li, T., Zhou, J., Chen, Y., Sheng, Z., Wang, Y., Yuan, X., 2016. Mesoporous silica derived from kaolin: Specific surface area enlargement via a new zeolite-involved template-free strategy. Appl. Clay Sci. 123, 76-82.

Shu, Z., Li, T., Zhou, J., Chen, Y., Yu, D., Wang, Y., 2014. Template-free preparation of mesoporous silica and alumina from natural kaolinite and their application in methylene blue adsorption. Appl. Clay Sci. 102, 33-40.

Skoronski, E., Souza, D.H., Ely, C., Broilo, F., Fernandes, M., Junior, A.F., Ghislandi, M.G., 2017. Immobilization of laccase from Aspergillus oryzae on graphene nanosheets. Int. J. Biol. Macromol. 99, 121-127.

Spina, F., Cordero, C., Schilirò, T., Sgorbini, B., Pignata, C., Gilli, G., Bicchi, C., Varese, G.C., 2015. Removal of micropollutants by fungal laccases in model solution and municipal wastewater: evaluation of estrogenic activity and ecotoxicity. J. Clean. Prod. 100, 185-194.

Sun, K., Huang, Q., Li, S., 2017. Transformation and toxicity evaluation of tetracycline

in humic acid solution by laccase coupled with 1-hydroxybenzotriazole. J. Hazard. Mater. 331, 182-188.

Tan, X., Liu, Y., Zeng, G., Wang, X., Hu, X., Gu, Y., Yang, Z., 2015. Application of biochar for the removal of pollutants from aqueous solutions. Chemosphere. 125, 70-85.

Tang, W., Zeng, G., Gong, J., Liang, J., Xu, P., Zhang, C., Huang, B., 2014. Impact of humic/fulvic acid on the removal of heavy metals from aqueous solutions using nanomaterials: A review. Sci. Total Environ. 468, 1014-1027.

Toor, M., Jin, B., Dai, S., Vimonses, V., 2015. Activating natural bentonite as a cost-effective adsorbent for removal of Congo-red in wastewater. J. Ind. Eng. Chem. 21, 653-661.

Wen, X., Du, C., Wan, J., Zeng, G., Huang, D., Yin, L., Deng, R., Tan, S., Zhang, J., 2019. Immobilizing laccase on kaolinite and its application in treatment of malachite green effluent with the coexistence of Cd (Π). Chemosphere. 217, 843-850.

Wu, H., Lai, C., Zeng, G., Liang, J., Chen, J., Xu, J., Dai, J., Li, X., Liu, J., Chen, M., Lu, L., Hu, L., Wan, J., 2017. The interactions of composting and biochar and their implications for soil amendment and pollution remediation: a review. Crit. Rev.

Biotechnol. 37, 754-764.

Xu, P., Zeng, G.M., Huang, D.L., Feng, C.L., Hu, S., Zhao, M.H., Lai, C., Wei, Z., Huang, C., Xie, G.X., Liu, Z.F., 2012. Use of iron oxide nanomaterials in wastewater treatment: A review. Sci. Total Environ. 424, 1-10.

Xu, P., Zeng, G.M., Huang, D.L., Lai, C., Zhao, M.H., Wei, Z., Li, N.J., Huang, C., Xie, G.X., 2012. Adsorption of Pb(II) by iron oxide nanoparticles immobilized Phanerochaete chrysosporium: Equilibrium, kinetic, thermodynamic and mechanisms analysis. Chem. Eng. J. 203, 423-431.

Yang, C., Chen, H., Zeng, G., Yu, G., Luo, S., 2010. Biomass accumulation and control strategies in gas biofiltration. Biotechnol. Adv. 28, 531-540.

Yang, J., Lin, Y.H., Yang, X.D., Ng, T.B., Ye, X.Y., Lin, J., 2017. Degradation of tetracycline by immobilized laccase and the proposed transformation pathway. J. Hazard. Mater. 322, 525-531.

Yu, J.G., Zhang, J., 2010. A simple template-free approach to TiO2 hollow spheres with enhanced photocatalytic activity. Dalton T. 39, 5860-5867.

Zeng, G., Wan, J., Huang, D., Hu, L., Huang, C., Cheng, M., Xue, W., Gong, X., Wang, R., Jiang, D., 2017. Precipitation, adsorption and rhizosphere effect: The mechanisms

for Phosphate-induced Pb immobilization in soils−A review. J. Hazard. Mater. 339, 354-367.

Zhang, C., Lai, C., Zeng, G., Huang, D., Yang, C., Wang, Y., Zhou, Y., Cheng, M., 2016. Efficacy of carbonaceous nanocomposites for sorbing ionizable antibiotic sulfamethazine from aqueous solution. Water Res. 95, 103-112.

Zhang, C., Liu, L., Zeng, G., Huang, D., Lai, C., Huang, C., Wei, Z., Li, N., Xu, P., Cheng, M., Li, F., He, X., Lai, M., He, Y., 2014. Utilization of nano-gold tracing technique: Study the adsorption and transmission of laccase in mediator-involved enzymatic degradation of lignin during solid-state fermentation. Biochem. Eng. J. 91, 149-156.

Zhang, Y., Zeng, G.M., Tang, L., Chen, J., Zhu, Y., He, X.X., He, Y., 2015. Electrochemical Sensor Based on Electrodeposited Graphene-Au Modified Electrode and NanoAu Carrier Amplified Signal Strategy for Attomolar Mercury Detection. Anal. Chem. 87, 989-996.

Zhou, C., Lai, C., Huang, D., Zeng, G., Zhang, C., Cheng, M., Hu, L., Wan, J., Xiong, W., Wen, M., Wen, X., Qin, L., 2018. Highly porous carbon nitride by supramolecular preassembly of monomers for photocatalytic removal of

sulfamethazine under visible light driven. Applied Catalysis B: Environmental. 220, 202-210.

Zhou, C., Sun, T., Gao, Q., Alshameri, A., Zhu, P., Wang, H., Qiu, X., Ma, Y., Yan, C., 2014. Synthesis and characterization of ordered mesoporous aluminosilicate molecular sieve from natural halloysite. J. Taiwan Inst. Chem. E. 45, 1073-1079.

Zhou, X., Lai, C., Huang, D., Zeng, G., Chen, L., Qin, L., Xu, P., Cheng, M., Huang, C., Zhang, C., Zhou, C., 2018. Preparation of water-compatible molecularly imprinted thiol-functionalized activated titanium dioxide: Selective adsorption and efficient photodegradation of 2, 4-dinitrophenol in aqueous solution. J. Hazard. Mater. 346, 113-123.

Zhou, Z., Hartmann, M., Chmelka, B.F., Stucky, G.D., Stucky, G.D., Weidinger, I.M., Scheller, F.W., Hildebrandt, P., Wollenberger, U., Park, J., Shi, C., Kim, J., Hyeon, T., Hyeon, T., Ha, S., Jung, H., Kim, J., 2013. Progress in enzyme immobilization in ordered mesoporous materials and related applications. Chem. Soc. Rev. 42, 3894.

Ztrk, N., Tabak, A., Akgl, S., Denizli, A., 2008. Reversible immobilization of catalase by using a novel bentonite-cysteine (Bent-Cys) microcomposite affinity sorbents. Colloids and Surfaces A: Physicochemical and Engineering Aspects. 322, 148-154.

Figure Captions

Fig. 1. Schematic of BDMMs preparation and succeeding laccase physisorption immobilization on BDMMs.

Fig. 2. SEM images and related EDS of a) bentonite, b) BDMMs, c) BDMMs-Lac, and d) BDMMs-Lac after TC degradation..

Fig. 3. A) BET nitrogen adsorption/desorption plots of the bentonite and BDMMs. B) FT-IR spectra of bentonite, BDMMS, BDMMS-Lac, and BDMMs-Lac after degradation. C) XRD curves of the bentonite and BDMMs.

Fig. 4. A) Effect of laccase concentrations from 0.5 mg/mL to 4 mg/mL on the activity of the immobilized laccase. B) Effect of time from 15 min to 180 min on the activity of the immobilized laccase. C) Effect of pH from 3.0 to 8.0 on the activity of the free and immobilized laccase.

Fig. 5. A) Operational stability of BDMMs-Lac in continuous cycles. B) Thermal stability studies of free laccase and BDMMs-Lac at 303-353 K for up to 120 min.

Fig. 6. A) Time-course of the removal and adsorption rates for TC by BDMMs-Lac and the heated-devitalized BDMMs-Lac. B) Effect of immobilized laccase dosage on the removal rates of TC by BDMMs-Lac.

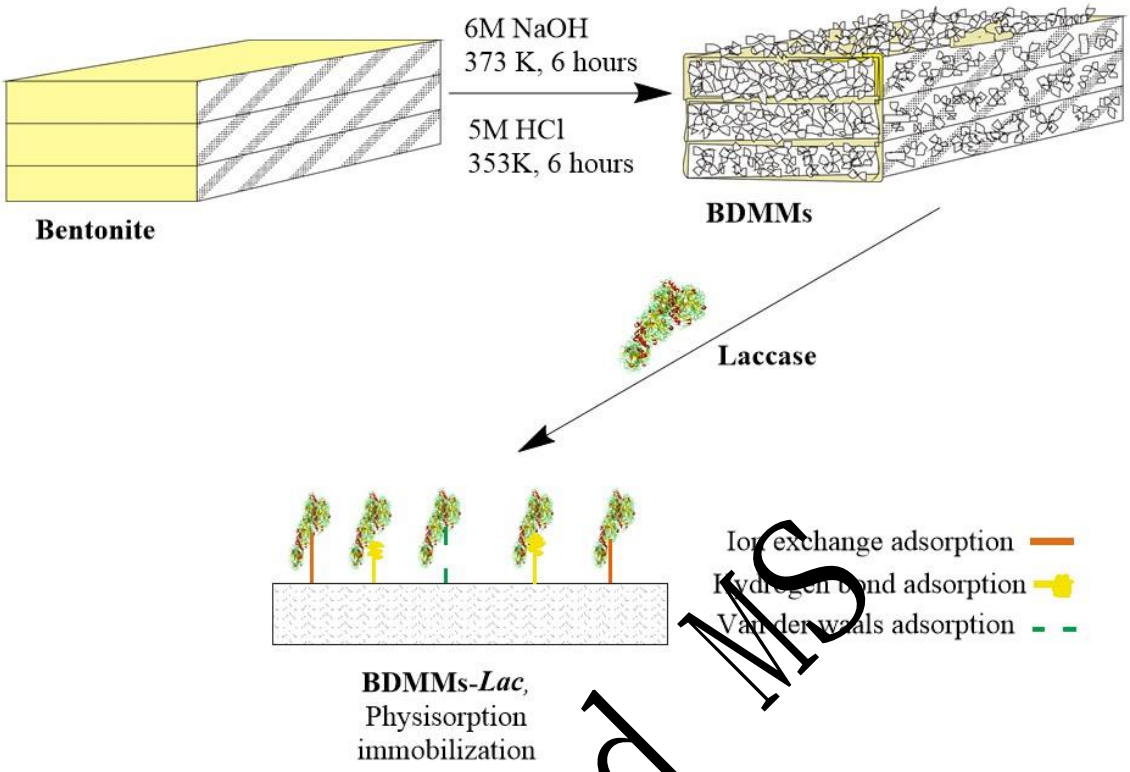

555

556 **Fig. 1**. Schematic of BDMMs preparation and succeeding laccase physisorption immobilization on

557 BDMMs.

558

559

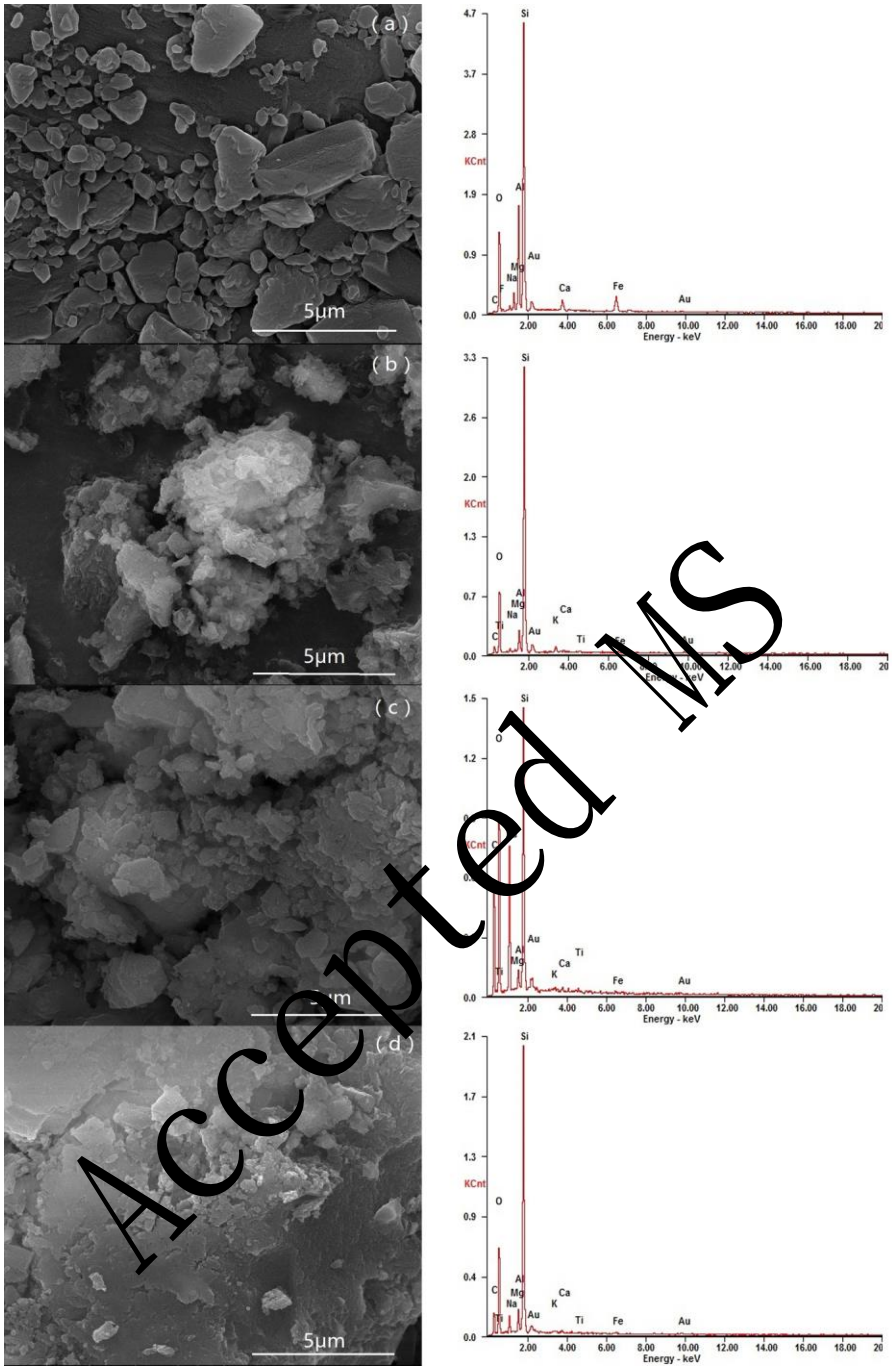

560

561 **Fig. 2**. SEM images and related EDS of a) bentonite, b) BDMMs, c) BDMMs-Lac, and d)

562 BDMMs-Lac after TC degradation..

563

564

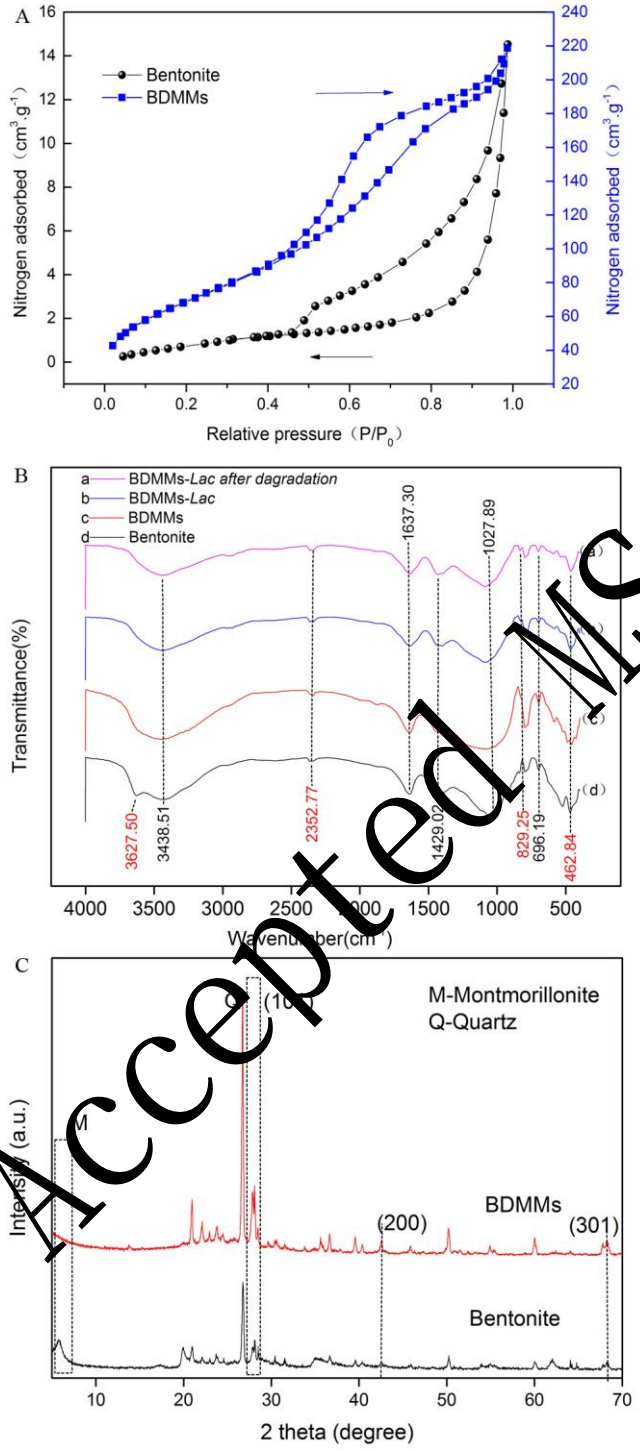

565

566 **Fig.3.** A) BET nitrogen adsorption/desorption plots of the bentonite and BDMMs. B) FT-IR spectra

567 of bentonite, BDMMS, BDMMS-Lac, and BDMMs-Lac after degradation. C) XRD curves of the

568 bentonite and BDMMs.

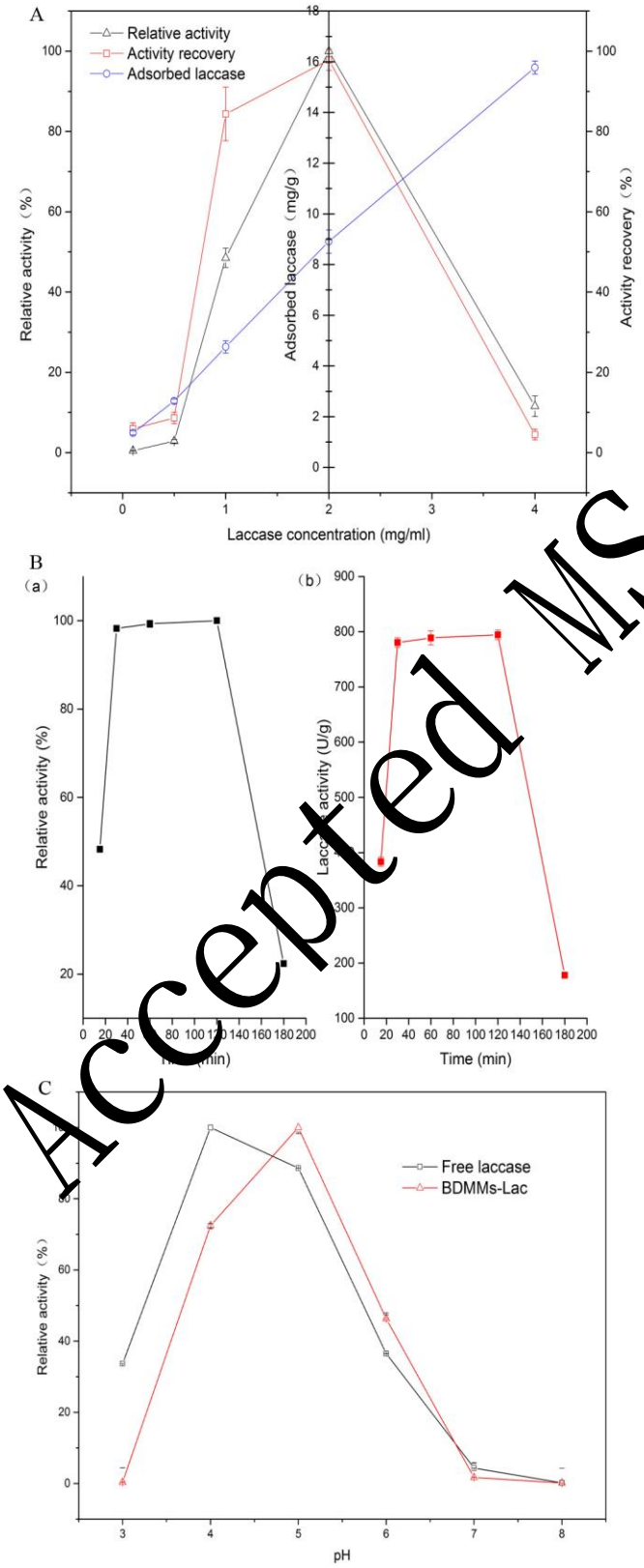

569

570 **Fig. 4**. A) Effect of laccase concentrations from 0.5 mg/mL to 4 mg/mL on the activity of the

571 immobilized laccase. B) Effect of time from 15 min to 180 min on the activity of the immobilized

572 laccase. C) Effect of pH from 3.0 to 8.0 on the activity of the free and immobilized laccase..

573

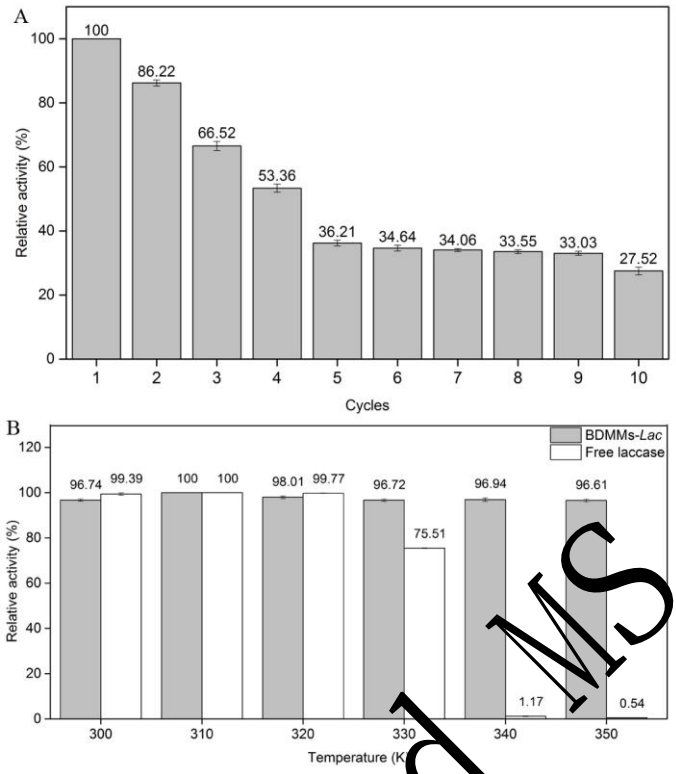

574

575 **Fig. 5**. A) Operational stability of BDMMs-Lac in continuous cycles. B) Thermal stability studies of

576 free laccase and BDMMs-Lac at 303-353 K for up to 120 min.

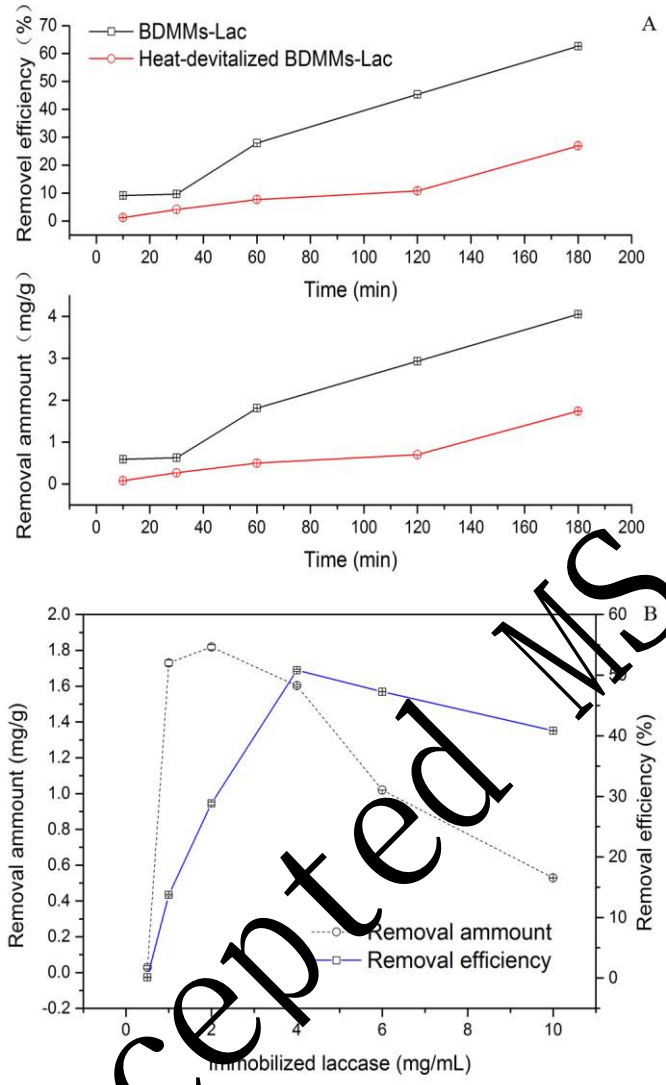

577

578 **Fig. 6**. A) Time-course of the removal and adsorption rates for TC by BDMMs-Lac and the

579 heated-devitalized BDMMs-Lac. B) Effect of immobilized laccase dosage on the removal rates of

580 TC by BDMMs-Lac.

581